

# ABSTRACT

We present a preliminary analysis of new X-ray data available for quasars, in the context of the 4DE1 Eigenvector 1 parameter space. 4DE1 serves as a surrogate H-R diagram for representing empirical diversity among quasars and for identifying the physical drivers of the diversity along a quasar "main sequence". The soft X-ray spectral index ( $\Gamma_{SOFT}$ ) was adopted as one of the principal 4DE1 correlates for contrasting extremes among Type 1 quasars. It partially motivated the hypothesis of two quasar populations (A and B) representing sources radiating at Eddington ratio  $L/L_{EDD}$  above and below  $\sim 0.15$  respectively. An X-ray trend was initially based upon ROSAT and ASCA data but we now confirm this dichotomy with large samples of X-ray spectra obtained with XMM and SWIFT. One popular idea connects the soft excess in Pop A quasars as a signature of thermal emission from a geometrically thick accretion disk in highly accreting sources radiating close to the Eddington limit.

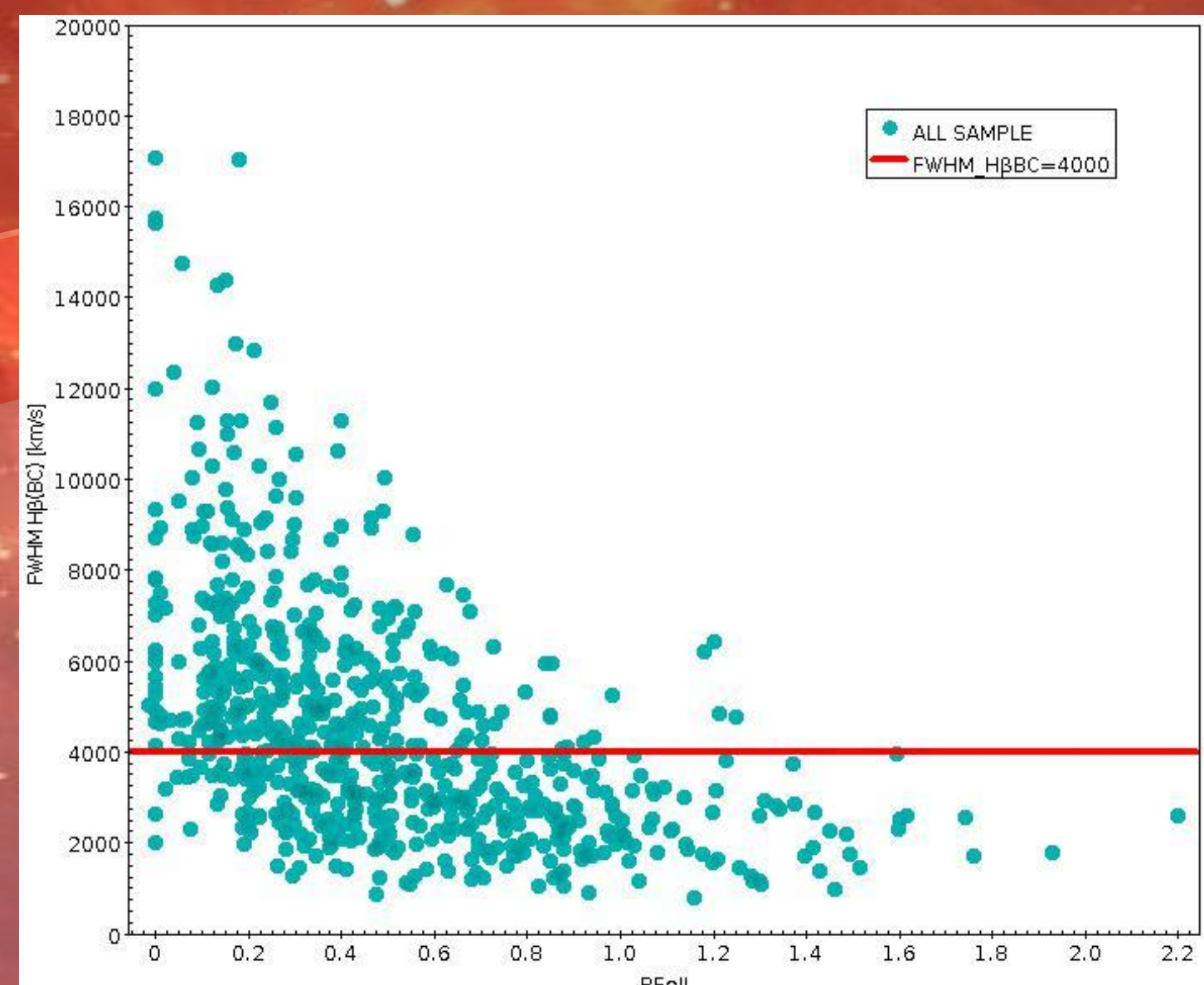
# SAMPLE

Our sample was built including all the Type 1 Quasars with accurate measurements of the lines involved in the 4DE1 optical scheme and with  $z < 0.8$ . In order to characterise the optical properties of quasar we explored the spectral information provided in Zamfir et al. (2010), Sulentic et al. (2007) and Marziani et al. (2003). We used 4DE1 parameter space measures of FWHM  $H\beta_{BC}$  (broad line) and the optical FeII blue blend ( $R_{FeII} = W(FeII\ 4570)/W(H\beta_{BC})$ ). These are the parameters that describe the optical plane of 4DE1. The sample of Zamfir consists of  $\sim 470$  low-redshift quasars with the highest S/N spectra extracted from SDSS DR5. The Marziani database includes 215 type 1 AGNs/radio galaxy nuclei and low-z quasars. The data from Sulentic involves 130 sources from the HST archive for which reliable C IV  $\lambda 1549\text{\AA}$  properties could be measured. Our final sample is consisted of 690 objects.

# POPULATIONS A & B QUASARS

Following the classification of Sulentic et al. (2000a & 2000b) we divided our sample into two groups based on FWHM  $H\beta_{BC}$ : Population A (FWHM  $H\beta_{BC} \leq 4000 \text{ km s}^{-1}$ ) and Population B (FWHM  $H\beta_{BC} > 4000 \text{ km s}^{-1}$ ). We show in the Figure 1 the location of the quasars of the sample in the optical plane of the 4DE1 parameter space, where the red horizontal line marks the boundary between the two populations.

Figure 1



# The Soft X-ray Excess in Active Galactic Nuclei

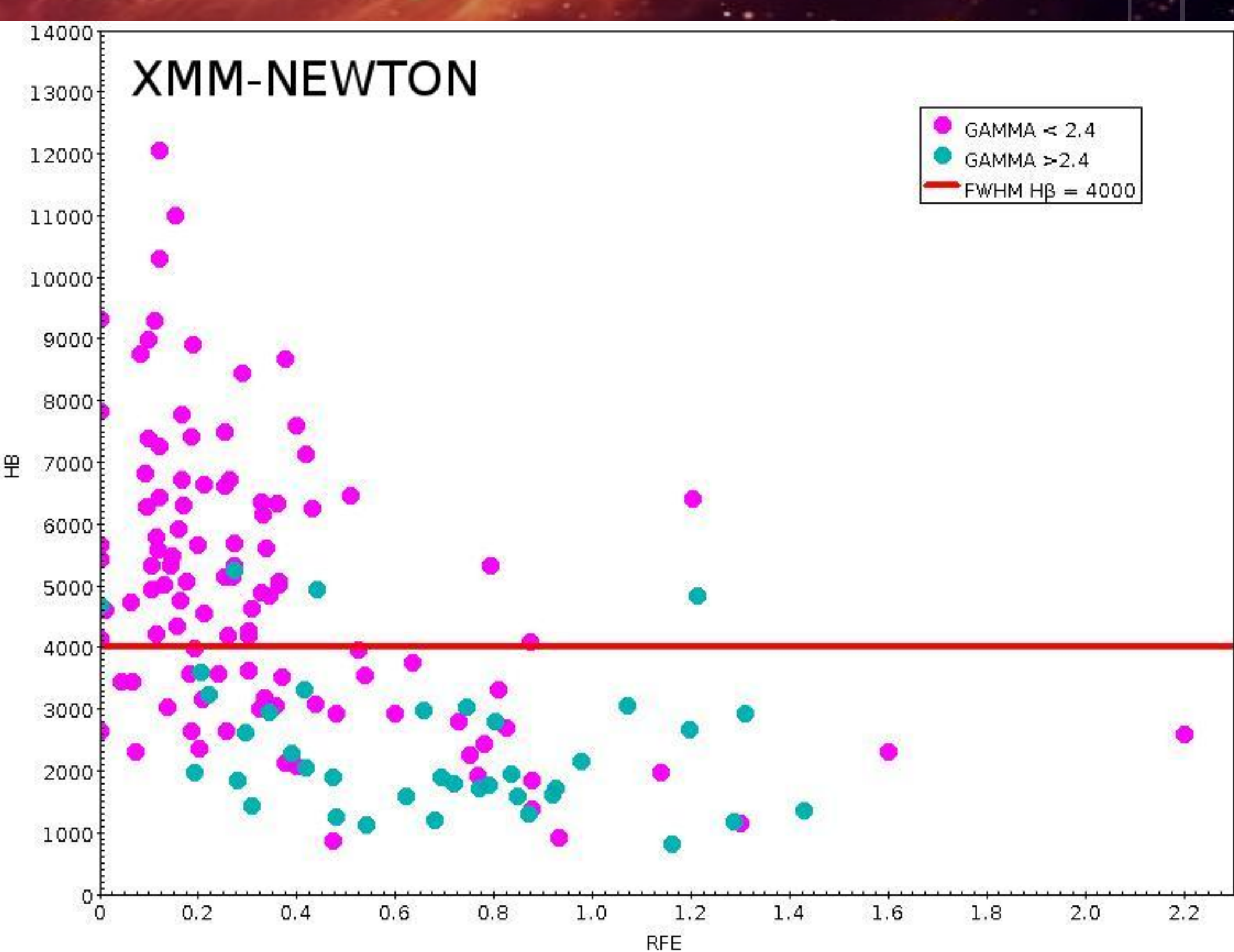
Katarzyna Bensch<sup>1</sup>  
A. del Olmo<sup>1</sup>, J. Sulentic<sup>1</sup>, J. Perea<sup>1</sup>, P. Marziani<sup>2</sup>

<sup>1</sup>Instituto de Astrofísica de Andalucía (IAA-CSIC), Spain  
<sup>2</sup>INAF Oss. Astronomico Padova, Italy

## C IV $\lambda 1549$ STUDY

The previous study carried out by Sulentic et al. (2007) addressed inter alia the problem of spectroscopic discrimination of the A & B populations. It involved the expanded sample of all low z quasars with HST/FOS UV spectra which allow to measure the C IV  $\lambda 1549\text{\AA}$ . The study showed that profile shift at half-maximum of high ionization C IV  $\lambda 1549\text{\AA}$  line constitutes the UV Eigenvector 1 measurement in the 4DE1 parameter space.

Figure on the left shows the optical plane of 4DE1 using colour to add the third 4DE1 UV parameter-the shift at half maximum of the C IV line from the rest frame. In this figure the color of the symbol indicates whether the C IV profile shows a blueshift or a redshift and the symbol size reflects the amplitude of the shift. Grey squares correspond to no significant line shift. Many C IV  $\lambda 1549$  profiles show a blueshift exceeding 1000 km/s (largest blue full circles) indicating a significant outflow or wind in such sources. Blueshifts increase with the Eddington ratio along the 4DE1 plane and clearly favor the Population A region (Sulentic et al. 2014).



# NEW X-RAY DATA

We matched our sample with the XMM and SWIFT X-ray databases. We allowed a maximum difference between optical and X-ray positions of 6 and 5.5 arcsec for XMM-Newton and SWIFT data, respectively. We collected X-ray spectral information into an X-ray database. Table 1 contains the numbers of X-ray sources which satisfied our selection criterion.

## XMM - NEWTON

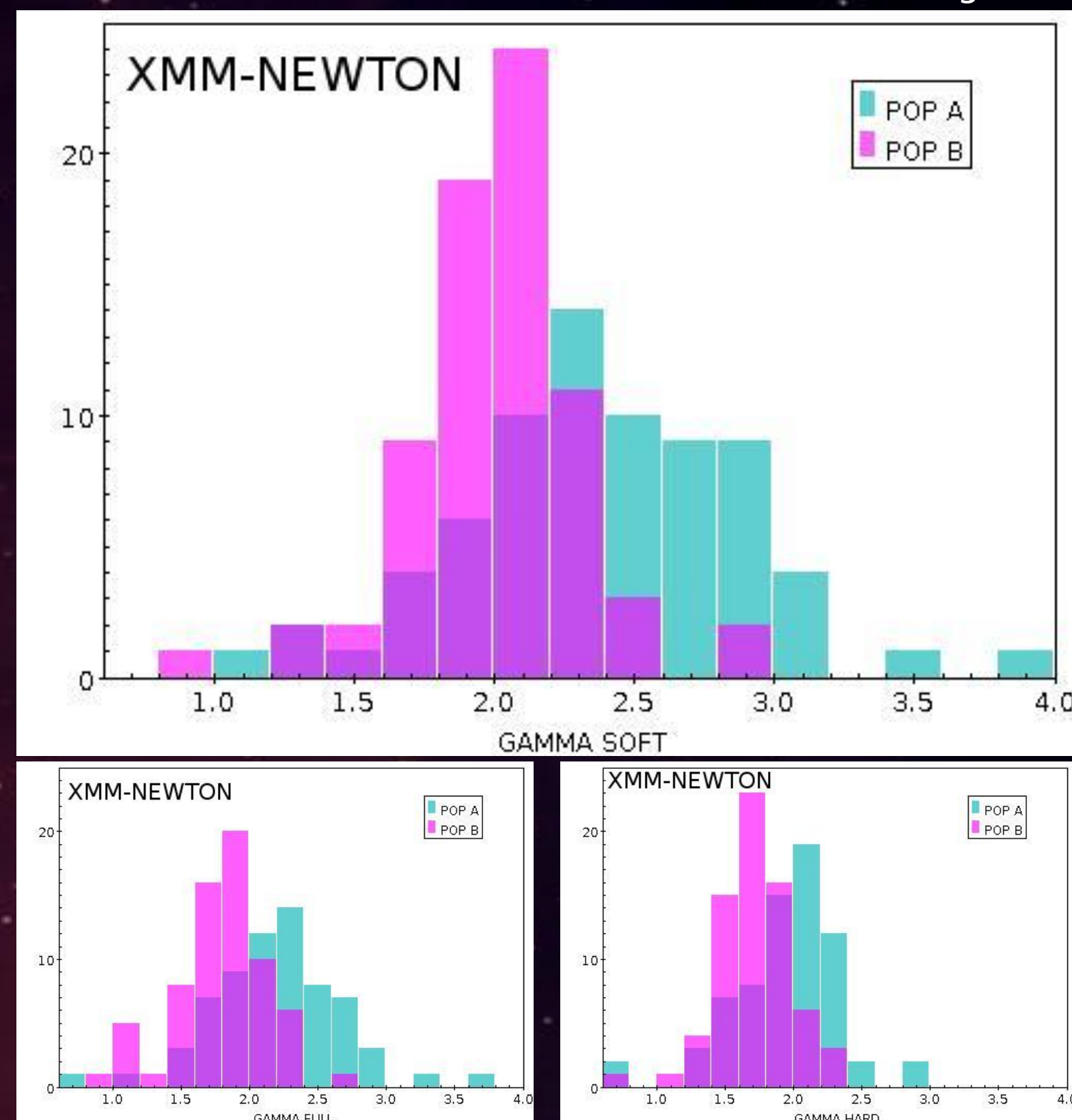
The XMM-Newton database, XMMFITS: The XMM-Newton spectral-fit database (Corral et al. 2015), provides us with information about the spectral slope for sources observed with the EPIC pn and MOS instruments. Photon indices ( $\Gamma$ ) were derived for three energy bands: Soft (0.5-2 keV), Hard (2-10 keV), and Full (0.5-10 keV). XMMFITS provides results of fitting XMM-Newton spectra with six models. We adopted values of  $\Gamma$  derived from fits using the absorbed power-law model for Full, Soft and Hard bands. The goodness of fit estimates enabled us to extract only the highest confidence values of  $\Gamma$ .

The histograms in the Figure 2 (on the right) compares the distributions of  $\Gamma$  for populations A and B. Values of  $\Gamma$  presented here were obtained by fitting the power-law models to Soft band - 143 sources (top), Full band - 143 sources (bottom left) and the Hard band - 140 sources (bottom right) for XMM spectra.

Table 1: Number of sources detected in X-rays

Parameter	Matches	Energy range [keV]
XMM-N		
$\Gamma_{FULL}$	146	0.5 - 10.0
$\Gamma_{SOFT}$	146	0.5 - 2.0
$\Gamma_{HARD}$	143	2.0 - 10.0
SWIFT		
$\Gamma_{FULL}$	214	0.3 - 10.0

Figure 2



## SWIFT

In order to provide spectral information from SWIFT we used data from the SWIFT X-ray Telescope point-source catalog (1SXPS, Evans et al. 2014). Spectral properties derived using three following methods are presented in the catalog: fixed spectra, interpolation of the HR values, and spectral fitting. We used the values of  $\Gamma$  obtained from fitting the absorbed power-law model in the energy range of 0.3 - 10 keV. We found that  $\Gamma_{FULL}$  provided by 1SXPS seems to be also a discriminator between the two populations A&B. Figure 3 presents a comparison of distribution of  $\Gamma_{FULL}$  measures derived from SWIFT spectra for population A and population B.

Figure 3

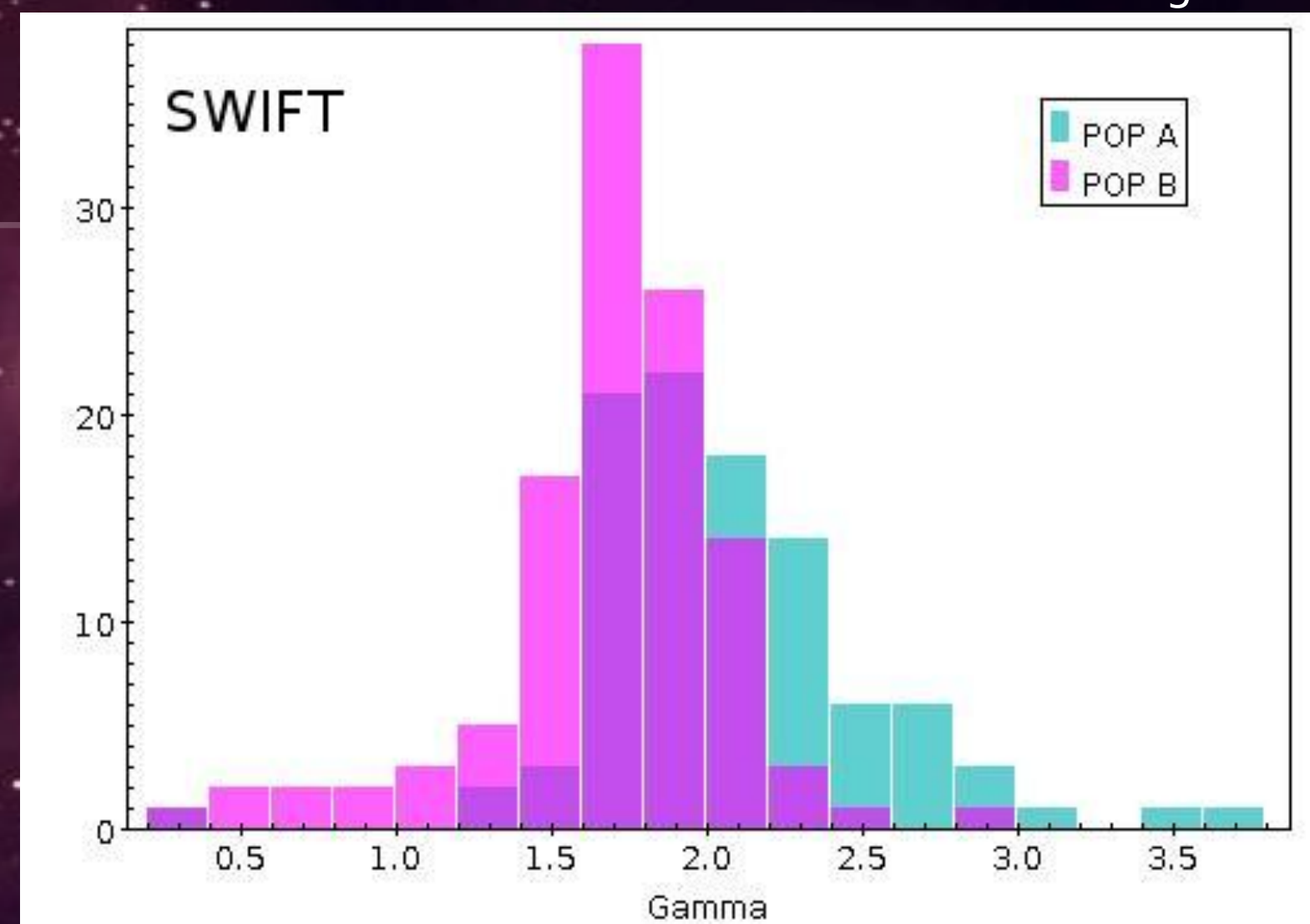


Figure 4

## SWIFT vs XMM

We expected the best separation of Pop A & B in distribution of  $\Gamma_{SOFT}$  since that  $\Gamma_{SOFT}$  is not available from Swift data we have compared XMM-Newton  $\Gamma_{SOFT}$  values and SWIFT  $\Gamma_{FULL}$  measures for the sources in common ( $\sim 80$ ). As can be seen in Figure 4 there is good relation between the values from both instruments. Therefore we use the values of  $\Gamma_{FULL}$  from SWIFT as a confirmation of our results of XMM-Newton. Figure 4 shows values of  $\Gamma_{SOFT}$  from XMM-Newton versus values of  $\Gamma_{FULL}$  from SWIFT for the sources in common. Table 2 presents values of  $\Gamma_{FULL}$  from SWIFT.

Table 2: SWIFT X-ray spectral parameters for full sample

Parameter	Median	Quartile 1	Quartile 3	Sources
Pop A $\Gamma_{FULL}$	2.00	1.77	2.30	99
Pop B $\Gamma_{FULL}$	1.73	1.58	1.89	115

# X-RAY PROPERTIES OF POPULATIONS A & B

We present the X-ray spectral characteristics of the two populations A & B of quasars included in our sample. Table 3 gives statistical information (median value, quartile 1 and quartile 3) derived for the parameters of  $\Gamma_{FULL}$ ,  $\Gamma_{SOFT}$  and  $\Gamma_{HARD}$  provided by XMM-Newton database and  $\Gamma_{FULL}$  parameter from SWIFT catalog. All parameters were derived for population A and B separately. Population A and Population B are statistically very different, the probabilities of being drawn from the same parent population are very small in all cases (less to  $8 \times 10^{-6}$ ) as measured by a Kolmogorov-Smirnov test.

The results are also confirmed by the parametric Student's t-test, which give values for the t statistics of 5.4, 4.0, and 5.1 for XMM-Newton  $\Gamma_{SOFT}$ ,  $\Gamma_{HARD}$  and  $\Gamma_{FULL}$  respectively. In all cases the probability are smaller than  $1 \times 10^{-4}$ . It is to note that gamma soft makes better discrimination between both populations whereas gamma hard is more similar between both populations.  $\Gamma_{FULL}$  lies between but it discriminates at a level of probability of  $1.4 \times 10^{-6}$  as measured by t.

Table 3: XMM-NEWTON X-ray spectral parameters for full sample

Parameter	Median	Quartile 1	Quartile 3	Sources
Pop A				
$\Gamma_{FULL}$	2.18	1.81	2.42	73
$\Gamma_{SOFT}$	2.35	2.03	2.71	73
$\Gamma_{HARD}$	1.97	1.68	2.16	71
Pop B				
$\Gamma_{FULL}$	1.82	1.58	1.99	73
$\Gamma_{SOFT}$	2.01	1.87	2.17	73
$\Gamma_{HARD}$	1.68	1.53	1.89	72

# PRELIMINARY CONCLUSIONS

Differences in X-ray spectra between the two populations of quasars classified using optical and UV spectral measures are presented in this poster. We find clear and highly significant differences between Population A and B spectral properties. While not included in the original PCA studies it is clear that  $\Gamma_{SOFT}$  is an additional valuable diagnostic for separating high and low accreting AGN. Both XMM-Newton and Swift measures confirm the Pop. A-B difference. While there is some overlap ( $\sim 80$  sources) SWIFT measures involve  $\sim 130$  AGN not observed by XMM. Lower luminosity Type 1 AGN dominate both samples making it unclear if the X-ray dichotomy extends to high z quasars often 2-3dex higher  $L_{BOL}$  than the majority of sources in these samples.  $\Gamma_{SOFT}$  correlates strongly with C IV  $\lambda 1549\text{\AA}$  blueshift measures. Those measures become stronger among higher L sources leading us to also expect a stronger X-ray signature at high z.

Figure on the left presents the distribution of the value of  $\Gamma_{SOFT}$  (XMM-Newton) along the optical plane of the 4DE1. Highly accreting population A quasars tends to show larger values of  $\Gamma_{SOFT}$ .

References  
- Corral, A., Georgantopoulos, I., Watson, M. G. et al. 2015, A&A, 576, A61  
- Evans, P. A., Osborne, J. P., Beardmore, A. P. et al. 2014, ApJS, 210, 8  
- Marziani, P., Sulentic, J. W., Zamanov, R. et al. 2003, ApJS, 145, 199  
- Sulentic, J. W., Zwitter, T., Marziani, P., Dultzin-Hacyan, D. 2000a, ApJ, 536, L5  
- Sulentic, J. W., Marziani, P., Dultzin-Hacyan, D. 2000b, ARA&A, 38, 521  
- Sulentic, J. W., Bachev, R., Marziani, P. et al. 2007, ApJ, 666, 757  
- Sulentic, J. W., Marziani, P., Dultzin, D., D'Onofrio, M., del Olmo, A. 2014, J PhCS, 565, 2018  
- Zamfir, S., Sulentic, J. W., Marziani, P., Dultzin, D. 2010, MNRAS, 403, 1759